CHAPTER 47

OBSERVATIONS OF WIND WAVE NONLINEARITY

T. H. C. Herbers and R. T. Guza

Center for Coastal Studies, A-009,
Scripps Institution of Oceanography,
La Jolla, California 92093, U.S.A.

Abstract

Observations of pressure fluctuations at the sea floor in 13 m depth are compared to an existing theory for weakly nonlinear surface gravity waves (Hasselmann, 1962). In this depth, free surface waves (obeying the dispersion relation) at sea and swell frequencies (0.05 - 0.3 Hz) are weakly attenuated, but free waves at frequencies higher than about 0.4 Hz do not reach the sea floor. However, nonlinear interactions between (primary) free waves of about the same frequency, propagating in nearly opposing directions, theoretically excite long wavelength, double frequency (secondary) forced waves that are only weakly attenuated at the sea floor. Bottom pressure spectra observed in 13 m depth show an ($O(10^2)$) increase in high frequency (0.35 - 0.6 Hz) forced wave energy levels in only a few hours after a sudden large veering in wind direction. Estimates of the free wave frequency-directional spectrum show a correspondingly rapid change with unidirectional seas when forced wave energy levels are low before the wind veering, and two nearly directionally opposing seas (0.15-0.3 Hz) when forced wave energy levels are high, consistent with the theoretical generation mechanism. The observed forced wave energy levels are in good agreement with theoretical predictions based on the directional spectrum estimates. Estimates of average wave numbers verify that sea and swell obey the dispersion relation, and show that double sea frequency forced waves have longer wavelengths than the interacting free waves, consistent with theory. Observed third order statistics confirm that the double frequency forced waves are coupled to the directionally opposing seas with a phase relationship predicted by theory.

Introduction

Wind generated surface gravity waves can be represented approximately by a linear superposition of statistically independent wavelets obeying the linearized equations (e.g., Kinsman, 1965). Observations presented here concern some of the weak, but interesting, nonlinear properties of natural wind waves. Theories for weakly nonlinear surface gravity waves, based on a perturbation expansion for small wave steepness, have been developed by various authors (Phillips, 1960; Hasselmann, 1962; and others). The lowest order wave

field is a frequency-directional spectrum $E(f,\theta)$ of free linear waves obeying the dispersion relation

$$f = \frac{1}{2\pi} [g \, |\mathbf{k}| \, \tanh(|\mathbf{k}| \, h)]^{\frac{1}{2}} \qquad (1)$$

where $\mathbf{k}$ is the vector wave number, h the water depth and g the acceleration of gravity. At the next order, forced (i.e., not obeying Eq. 1) secondary waves are generated in nonresonant triad interactions with two free wave components. Each pair of primary (free) waves, with frequencies and wave numbers $(f_1,\mathbf{k}_1)$ and $(f_2,\mathbf{k}_2)$, is accompanied by a pair of secondary waves with the sum and difference frequency and wave number $(f_1 \pm f_2, \mathbf{k}_1 \pm \mathbf{k}_2)$. These lowest order nonlinearities theoretically result in weakly nonGaussian statistics and possibly large deviations from the dispersion relation (e.g., Phillips, 1960; Hasselmann et al., 1963). For example, if $E(f,\theta)$ is narrow and unimodal, then the dominant secondary wave contribution to sea surface elevation is due to the interactions of free wave components with nearly equal frequency $(f_1 \approx f_2)$ and wave number $(\mathbf{k}_1 \approx \mathbf{k}_2)$. The sum interaction yields the familiar $(2f, 2\mathbf{k})$ Stokes forced wave, in phase with the free wave components, that theoretically distorts the sinusoidal linear wave surface to a profile with sharper crests and flatter troughs. The Stokes correction, which in deep water has double the wavelength of a free wave with the same frequency, contributes a positive skewness to sea surface statistics.

At great depth the theoretically expected local nonlinear effects are markedly different than at the sea surface. Surface gravity waves (both free and forced components) are very strongly attenuated at depths below the sea surface that exceed about half their wavelength. Free waves obeying the dispersion relation (Eq. 1) with typical sea and swell frequencies (0.05-0.3 Hz) are therefore confined to the upper 10-300 m of the ocean, as are the Stokes-type $(2f, 2k)$ secondary waves. Forced waves, however, can have very long wavelengths if $\mathbf{k}_1 \approx \pm \mathbf{k}_2$ and penetrate virtually unattenuated to the ocean floor. A long wavelength, double frequency forced wave ($2f, k \approx 0$) can be generated by the sum interaction of two free waves of nearly equal frequency travelling in opposing directions $(f_1 \approx f_2, \mathbf{k}_1 \approx -\mathbf{k}_2$, Miche, 1944). This nonlinear effect is believed to cause high frequency sea floor pressure oscillations and microseisms in the deep ocean (e.g., Longuet-Higgins, 1950).

The present study examines the properties of high frequency secondary forced waves in natural wind waves. Array measurements of wave pressure were collected offshore of Chesapeake Bay in a water depth of 13 m. In this depth locally generated seas (0.15-0.3 Hz) are only weakly attenuated at the sea floor while free waves at double sea frequencies (> 0.35 Hz) are very strongly attenuated, so that relatively weak (at the sea surface) double sea frequency forced waves with longer wavelengths are theoretically dominant at the sea floor. The present observations show, in agreement with theory, that long wavelength high frequency forced waves are generated by the sum interactions of seas travelling in nearly opposing directions. The experiment is described in section 2. In section 3, frequency spectra of pressure on the sea floor are presented that show a rapid increase in forced wave energy levels at double sea frequencies after a large veering in local wind direction, as a result of the nonlinear interactions of nearly directionally opposing seas. The observed energy levels of forced waves are consistent with weakly nonlinear theory. In section 4, deviations from the dispersion relation and nonGaussian statistics associated with weakly nonlinear waves are examined with estimates of average wave numbers and third order

statistics of the bottom pressure field. The results are summarized in section 5. A full account of the observations is given in Herbers and Guza (1990 b, c).

Experiment

   Arrays of pressure transducers were deployed at the Chesapeake Light Tower, as part of the SAXON (SAR and X-band Ocean Nonlinearities) experiment. The tower is situated on an exposed shoal approximately 30 km offshore of Cape Henry, Virginia, U.S.A.. The water depth at the tower is 13 m with approximately 0.5 m tidal fluctuations. Two arrays were deployed, each consisting of seven capacitance sensing pressure transducers. One of the arrays (dimensions 20 m x 20 m) was mounted on the tower structure at mid-depth and the other array (dimensions 12 m x 12 m) on the seabed (Fig. 1). The primary purpose of the mid-depth array was to provide estimates of the frequency-directional spectrum $E(f, \theta)$ of (free) sea and swell. The bottom array was deployed to measure the secondary pressure
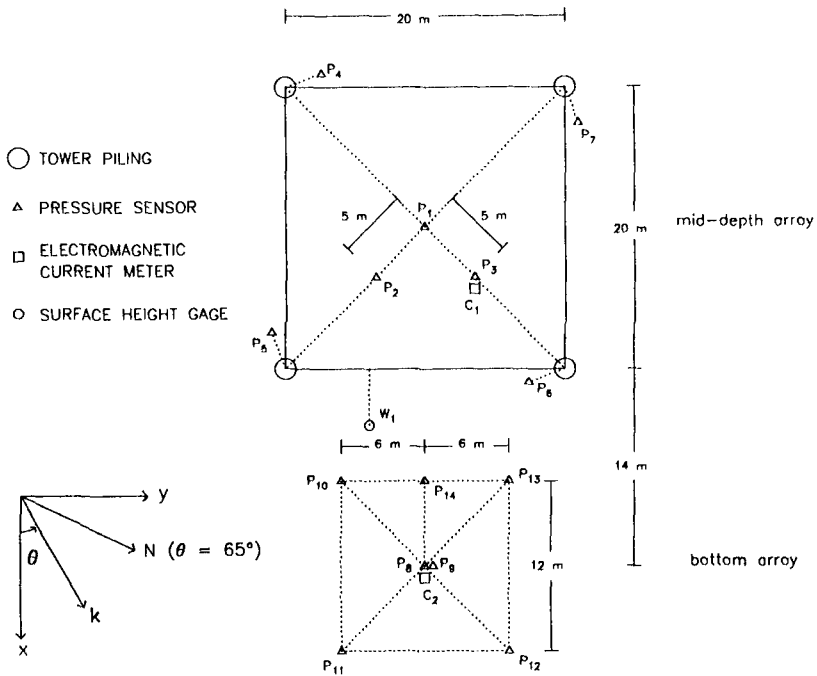

Figure. 1.   Plan view of mid-depth (6 m below Mean Sea Level) and bottom (13 m below Mean Sea Level) array geometries and analysis coordinate frame. k is the wave number vector and θ is the wave propagation direction. $\theta = 65°$ corresponds to waves arriving from the South.

field. It is better suited for detecting weak high frequency forced waves than the mid-depth array because high frequency free waves are more strongly attenuated at the sea floor than at mid-depth. The bottom array was displaced approximately 24 m East from the center of

the tower (Fig. 1) to reduce tower interference, all bottom sensor locations were accurate to within 5 cm, and the sensors were buried about 10 cm in the sand to reduce flow noise. Data was collected with a 2 Hz sample frequency on a nearly continuous basis from 17 September through 14 October, 1988, spanning a wide range of conditions. Surface elevation data (sampled at 30 Hz) from a surface piercing wire gage, located on the East side of the tower (Fig. 1), was collected intermittantly by A. T. Jessup (1989, personal communication). Throughout the experiment the predominantly tidal mean flows, observed at mid-depth and on the bottom, were smaller than about 25 cm/sec and their effect is negligible.

3. Forced Wave Energy and Directionally Opposing Seas

Fig. 2 shows the evolution of the average (over all bottom sensors) bottom pressure frequency spectrum $E_b(f)$ during a 85 hour period, 9 through 13 October 1988. The local wind during this period was highly variable with moderate speeds less than 15 m/sec (Fig.
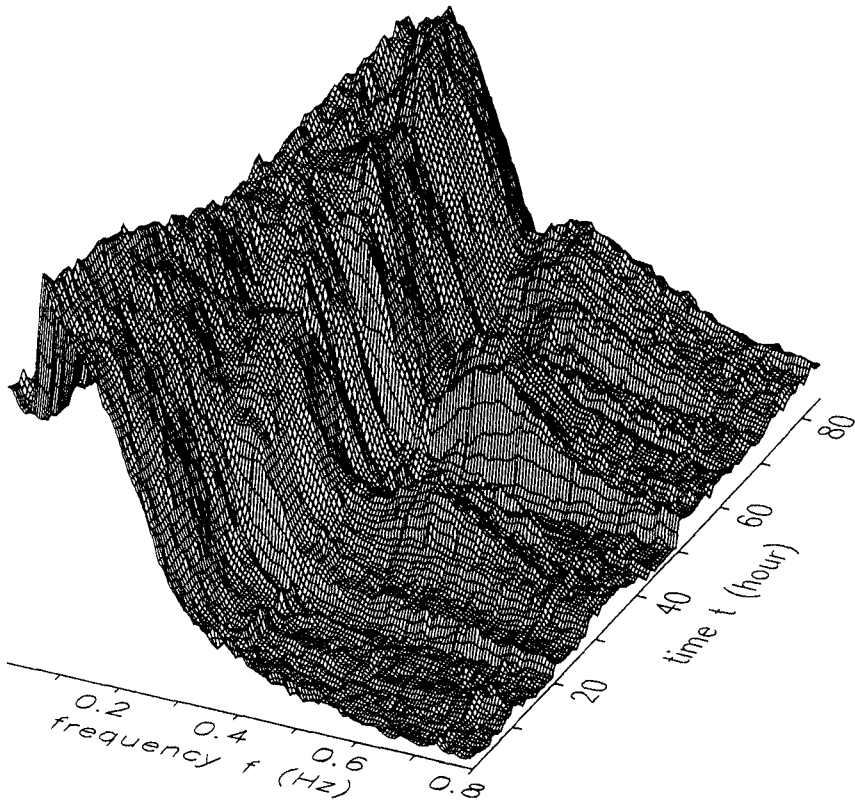

Figure 2.   A 3-dimensional surface of $\log E_b(f)$ from 9 October 20:30 h through 13 October 09:30 h, 1988 (local time) at hourly intervals.

3) and significant wave heights ranged from 0.5 to 1.5 m. The high variability in the bottom pressure spectra in the frequency range of 0.35 - 0.7 Hz is striking. In particular, between $t \approx 49$ and 53 h the energy in this range suddenly increases by more than 2 orders of magnitude and a broad feature develops with its peak at approximately 0.47 Hz (Fig. 4). The present study is focused on this event; Herbers and Guza (1990 b, c) discuss the entire period. These high frequency pressure fluctuations cannot be explained with linear wave theory because of the strong attenuation of high frequency free waves. For example, for a surface gravity wave component with frequency $f = 0.5$ Hz, that obeys the linearized equations, the attenuation of pressure at the sea floor relative to the surface is approximately 10^6. Sea surface excursions of $O(1 \text{ km})$ would be needed to generate free 0.5 Hz bottom pressure oscillations with $O(1 \text{ mm})$ amplitude (approximately the root mean square value of the high frequency pressure fluctuations at $t = 53$ h). Wave staff data and visual observations show significantly smaller seas.
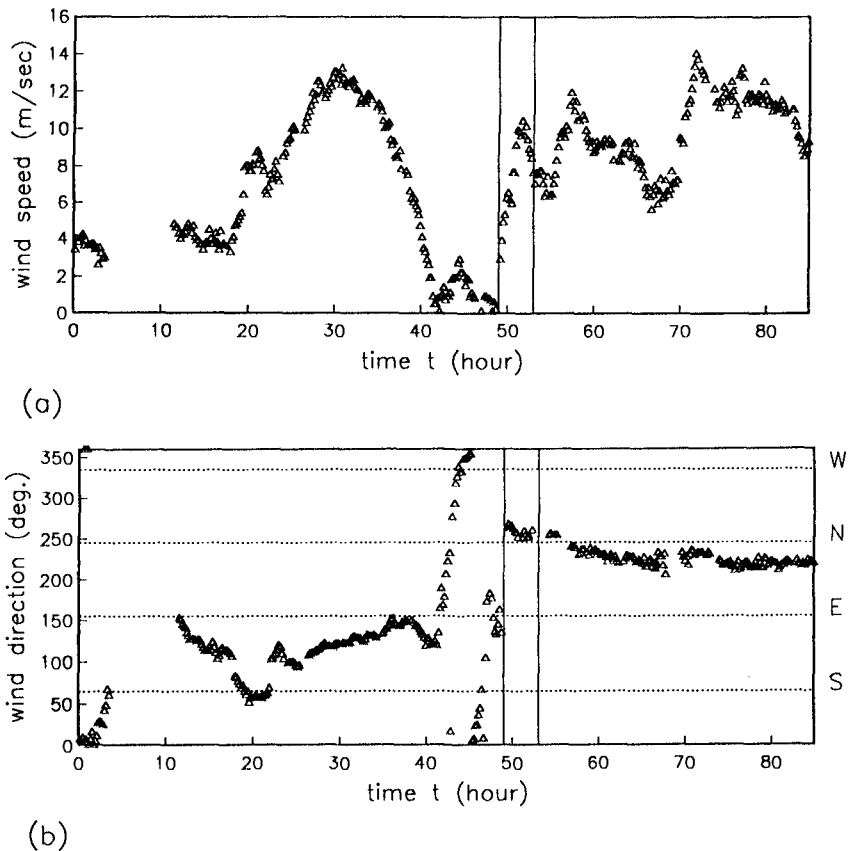

(a)

(b)

Figure 3.   Ten minute averages of wind speed (a) and direction (b) measured 42 m above the sea surface on top of the light tower (edited data provided by A.T. Jessup, personal communication). The vertical lines indicate times selected for detailed analysis.

Between t = 20 h and 40 h, the wind was relatively steady in direction from the South-East ($\approx 110°$) with speeds increasing from 4 m/sec to a maximum of 13 m/sec at t = 30 h and decreasing to near calm at t = 40 h (Fig. 3). During the period t = 40 - 50 h, the wind remained calm, followed by a rapid increase to about 10 m/sec at t = 50 h, with a direction from the North ($\approx 260°$) nearly opposing the wind direction 20 hours previous (Fig. 3). The dramatic increase in high frequency energy levels between t = 49 h and t = 53 h (Fig. 4) is related to this change in local winds, but the nonlinear interactions are more complicated than the familiar Stokes second harmonic corrections. In a narrow band surface elevation frequency-directional spectrum $E_s(f,\theta)$ with peak frequency f_p and peak direction θ_p, generation of high frequency secondary waves on the sea surface is dominated by the ("self-self") interactions of energetic components near the spectral peak ($f_1 \approx f_2 \approx f_p$, $\theta_1 \approx \theta_2 \approx \theta_p$). However, these $(2f_p,\theta_p)$ second harmonics have double the wave number k_p of the free wave components and are very strongly attenuated at the sea floor if $k_p h \gg 1$. For the present observations of local seas with periods of 4 to 5 sec in 13 m depth, $k_p h \approx 3$. Stokes self-self interactions in this relatively deep water are both weak at the sea surface (i.e., not amplified by near-resonance) and very strongly attenuated at the sea floor. Longer wavelength forced waves that are generated by the interactions of seas and swell propagating in (nearly) opposing directions are expected to dominate the secondary bottom pressure spectrum.
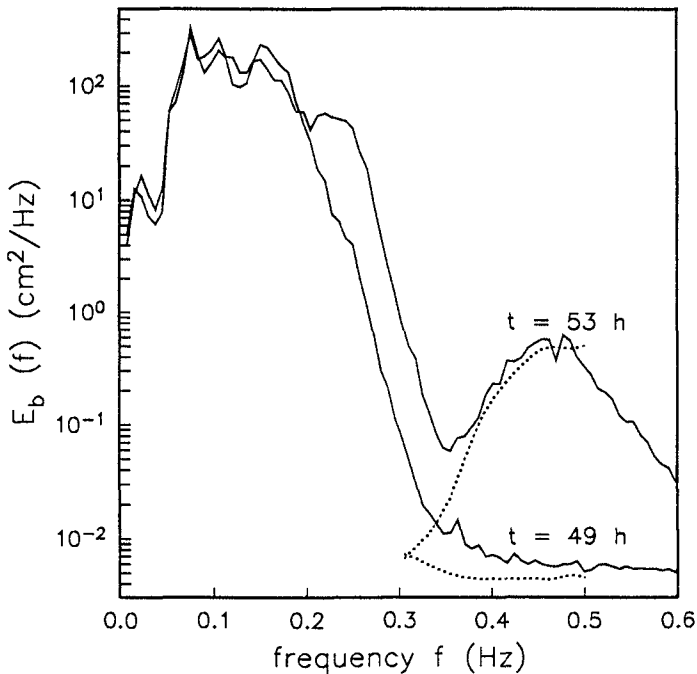

Figure 4.   Observed (solid, an average of all bottom sensors) and predicted (dotted, at double sea frequencies 0.3 - 0.5 Hz) bottom pressure frequency spectra, before and after a large increase in forced wave energy levels.

To verify that the observed forced waves are generated by directionally opposing seas, frequency-directional spectra $E_s(f,\theta)$ of free waves (i.e., obeying the dispersion relation, Eq. 1) were estimated from the mid-depth pressure array data. $E_s(f,\theta)$ is expressed as

$$E_s(f,\theta) = E_s(f)\, S(\theta;f) \qquad (2)$$

where $E_s(f)$ is the surface elevation frequency spectrum and $S(\theta;f)$ is the directional distribution at frequency f. On a frequency band by frequency band basis the "smoothest" $S(\theta)$ "consistent" with the array data is obtained by minimizing a roughness measure of the form

$$\int d\theta \left[\frac{d^2 S(\theta)}{d\theta^2} \right]^2$$

subject to the constraint that $S(\theta)$ is a nonnegative function with unit integral that fits the array cross-spectra within a 75 % confidence level (Herbers and Guza, 1990a). Fig. 5 shows estimates of $E_s(f,\theta)$, obtained from the mid-depth array cross-spectra (200 degrees of freedom), at $t = 49$ and 53 h in the frequency range 0.05 - 0.3 Hz, where the energy spectra are energetic and assumed to be dominated by free waves obeying the dispersion relation. This assumption is verified in section 4. At $t = 49$ h, when forced wave energy levels are low, the $E_s(f,\theta)$ estimate shows nearly unidirectional seas from the South with peak frequency 0.18 Hz (Fig. 5a). Four hours later (Fig. 5b), more energetic, slightly higher frequency ($f_p \approx 0.26$ Hz) locally generated seas arriving from the North are also present in a bimodal $E_s(f,\theta)$. The sudden, nearly $180°$ veering in wind direction from South to North between approximately $t = 40$ h and $t = 50$ h is consistent with the observed change in $E_s(f,\theta)$. Predictions of the forced wave bottom pressure spectrum in the frequency range 0.3 - 0.5 Hz, based on the two $E_s(f,\theta)$ estimates (Fig. 5) and weakly nonlinear theory (Hasselmann, 1962; see Herbers and Guza, 1990b, for the details of the calculations), are compared to the
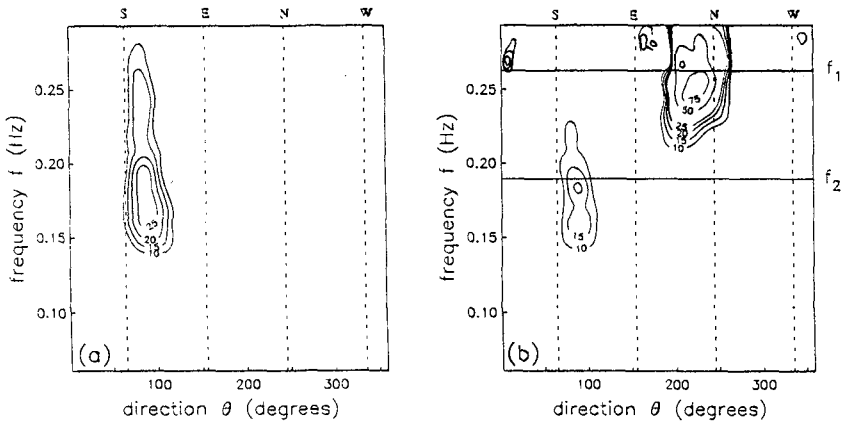

Figure 5.   Estimates of the surface elevation frequency-directional spectrum (units $cm^2/Hz°$) at $t = 49$ h (a) and 53 h (b). Solid lines (b) indicate bispectral peak frequencies (Fig. 8).

observed bottom pressure spectra (an average of all bottom sensors) in Fig. 4. At frequencies below 0.35 Hz the observed pressure spectrum shows increasingly more power than the forced wave prediction because free waves reach the sea floor. In the frequency range 0.35 - 0.5 Hz, predicted forced wave spectra show the dramatic increase in forced wave energy after the wind veered, due to the interactions of opposing seas, and are in good agreement with the observed forced wave energy levels. However, a change in local wind conditions is not the only mechanism for generation of directionally opposing seas and associated long wavelength forced waves. The double sea frequency forced wave peaks at $t \approx 32$ h and $t \approx 80$ h (Fig. 2) are generated by a similar change in the directional wave spectrum, but the bi-directional seas are the result of the arrival of nonlocally generated wind waves rather than a veering wind (Herbers and Guza, 1990b).

Fig. 6 shows the frequency spectra of all pressure sensors in the mid-depth and bottom array, and a surface elevation spectum computed from surface piercing wire gage data (provided by A.T. Jessup, personal communication) at t = 53 h. The observed vertical decay of sea and swell (0.05 - 0.3 Hz) is consistent with the dispersion relation for free waves (Herbers and Guza, 1990b). The relative decay between mid-depth and bottom pressure at the double sea frequency forced wave peak is not only much weaker than the theoretical value for linear waves but also weaker than the decay of the interacting seas, consistent with the long wavelengths of forced waves generated by opposing seas. As expected from theory, free wind generated waves dominate surface elevation at high frequencies but are very strongly attenuated below about mid-depth (at 0.5 Hz the predicted power decay of free waves at the mid-depth array, relative to the surface, is 10^{-5}). Forced
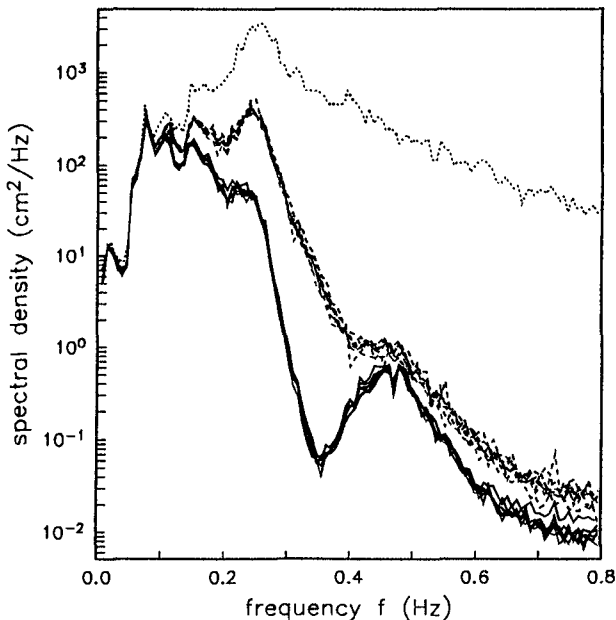

Figure 6.   Pressure frequency spectra on the sea floor (solid) and at mid-depth (dashed) at t = 53 h. The dotted line is a surface elevation spectrum (data provided by A.T. Jessup, personal communication).

waves smaller in amplitude, but with longer wavelengths, are only weakly attenuated and dominate the high frequency pressure field in the lower part of the water column.

4. Average Wave Numbers and Third Order Statistics

Secondary forced wave components cause nonGaussian statistics and deviations from the dispersion relation. Third order statistics of weakly nonlinear waves are nonzero owing to a statistically consistent phase relationship between free and forced wave components. The resulting nonzero skewness of the bottom orbital velocity field may be important to sediment transport on the shelf. The deviations of forced waves from the dispersion relation can be very large and cause errors in the interpretation of bottom pressure measurements which is often based on the linear dispersion relationship. This is true in particular at frequencies high enough that free waves are strongly attenuated and forced waves contribute significantly to the spectral density. In this section deviations from the dispersion relation and statistical coupling of free and forced waves are examined in the bottom pressure data at $t = 53$ h with high forced wave energy levels (Fig. 4).

A bulk averaged wave number $k_{rms}(f)$ defined as

$$k_{rms}(f)^2 \equiv \int d\mathbf{k} \ |\mathbf{k}|^2 \ E_b(f,\mathbf{k}) \Big/ \int d\mathbf{k} \ E_b(f,\mathbf{k}) \qquad (3)$$
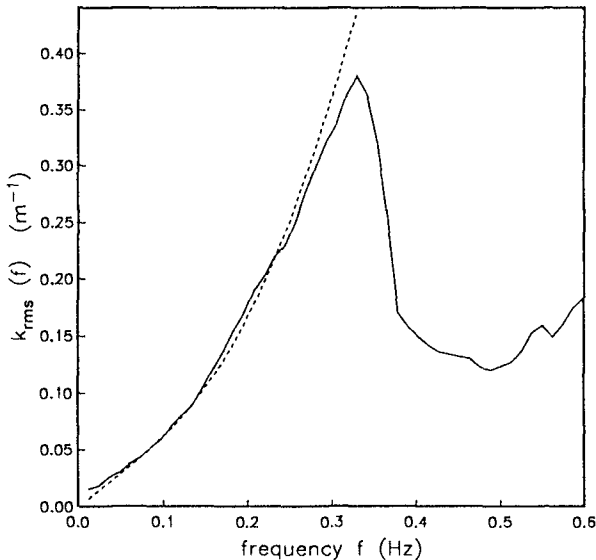

Figure 7.   A $k_{rms}(f)$ estimate at $t = 53$ h. The dashed curve is the surface gravity wave dispersion relation.

with $E_b(f,\mathbf{k})$ the bottom pressure wave number-frequency spectrum, can be estimated from a compact array of bottom pressure sensors with spacings L_{ij} small compared to the surface wavelength. The details of the technique, which utilizes a linear combination of the cross-spectral elements, are described in Herbers and Guza (1990c). Fig. 7 shows a $k_{rms}(f)$ estimate at $t = 53$ h. In the frequency range 0.05 - 0.3 Hz, the wave number estimate agrees with the linear dispersion relation within a few percent, consistent with the assumption (used when estimating $E_s(f,\theta)$, Eq. 2) that this part of the spectrum is dominated by free sea and swell. In the spectral valley between the wind wave and double frequency peaks $k_{rms}(f)$ drops sharply and reaches a minimum near the double sea frequency peak ($f \approx 0.5$ Hz). In fact the observed forced waves (that do not obey the dispersion relation) have longer wave lengths than the free waves forcing them, qualitatively consistent with the theory for forced waves excited by the observed directionally opposing seas (Fig. 5).

To examine statistical coupling between the directionally opposing sea peaks and the double frequency forced wave peak, bispectra (Hasselmann et al., 1963; Elgar and Guza, 1985; and others) were computed from the bottom pressure data. Fig. 8 shows an estimate of the normalized bispectrum $b(f_1,f_2)$

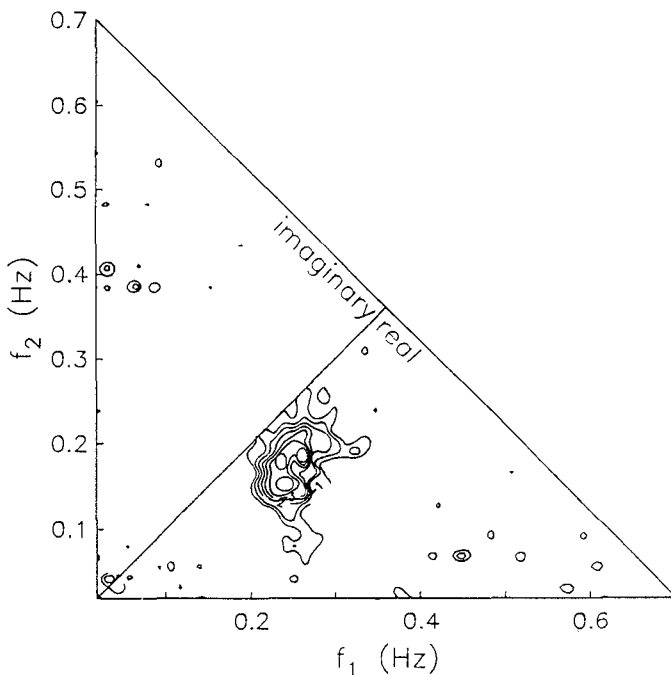$$b(f_1,f_2) \equiv \frac{B(f_1,f_2)}{[E_b(f_1)\,E_b(f_2)\,E_b(f_1+f_2)]^{\frac{1}{2}}} \qquad (4)$$

Figure 8.   A $b(f_1,f_2)$ estimate (spectra averaged over all bottom sensors) at $t = 53$ h. Contours at levels -6, -5, -4, -3, -2, 2, 3, 4, 5, and 6 $\mathrm{Hz}^{-\frac{1}{2}}$ are shown.

with the bispectrum $B(f_1, f_2)$ defined as the expected value of the third order moment of the bottom pressure Fourier-Stieltjes transform $dZ(f)$:

$$B(f_1, f_2)\, df_1\, df_2 \equiv 2\, \mathbf{E}\{dZ(f_1)\, dZ(f_2)\, dZ(-f_1-f_2)\} \qquad (5)$$

The bispectrum vanishes for the wind generated Gaussian free waves and statistically significant deviations of $b(f_1, f_2)$ from zero can be interpreted as nonlinearity of the bottom pressure field associated with the presence of forced waves. Theoretically, the contributions of triad interactions between f_1 (free), f_2 (free) and $f_1 + f_2$ (forced) wave components to $b(f_1, f_2)$ are real (Hasselmann et al., 1963), which means that the bottom pressure field is skewed (i.e., different crest and trough profiles) but statistically symmetric about a vertical plane (i.e., wave crests are not pitched forward or backward). In 13 m depth, the bispectrum at double sea frequencies is theoretically negative and these long forced waves may contribute to a negative skewness of sea floor pressure and orbital velocity fields, rather than the positive skewness of Stokes waves (Herbers and Guza, 1990b). Fig. 8 shows that the observed $b(f_1, f_2)$ is real (deviations of the imaginary part from zero are statistically insignificant), negative, and has a large peak centered at $f_1 \approx 0.26$ Hz, $f_2 \approx 0.18$ Hz. These frequencies are very close to the peak frequencies of the two directionally opposing wind wave systems (Fig. 5b). The observed bispectrum is thus consistent with the theoretical phase relationship between directionally opposing primary waves and secondary long waves (Herbers and Guza, 1990b). Integrals of $B(f_1, f_2)$ along constant sum frequency $f_1 + f_2$ (not shown here, discussed in Herbers and Guza, 1990c) show that nearly all of the wave energy in the range 0.4 - 0.5 Hz is statistically coupled to the two directionally opposing seas. The bispectral estimate thus provides an independent verification of the hypothesis that the observed forced waves are generated by directionally opposing seas.

5. Summary and Conclusions

To examine local nonlinear effects on natural wind generated surface gravity waves, arrays of pressure transducers were deployed at mid-depth and on the sea floor in 13 m deep water, approximately 30 km offshore of Cape Henry, Virginia. Bottom pressure data show enhanced energy at double sea frequencies that appears to be nonlinearly driven by local seas. These nonlinear bottom pressure observations are explained using an existing theory for weakly nonlinear waves (e.g., Hasselmann, 1962). The perturbation solution to second order in wave steepness consists of (primary) free waves obeying the dispersion relation and (secondary) forced waves that do not obey the dispersion relation, generated by interactions between pairs of free waves. Free and forced wave components are both strongly attenuated at depths exceeding about half a wavelength, but forced waves excited by the interactions of directionally opposing free waves of nearly equal frequency have much longer wavelengths than free waves of the same frequency, and thus penetrate to greater depths. In narrow band directional spectra the dominant nonlinear interactions at the sea surface are between waves near the spectral peak having nearly equal frequency and propagation direction. However, in 13 m depth the bottom pressure energy levels of "Stokes harmonics" at double sea frequencies are strongly attenuated, approximately 10^4–10^6 weaker than the energy levels of relatively unattenuated forced waves generated by two narrow seas of equal frequency and energy, travelling in nearly opposing directions. Forced wave energy levels on the sea floor in 13 m depth at double sea frequencies are thus theoretically expected to be weak in unidirectional seas and increase dramatically when directionally opposing seas are present.

After the local wind veered, the observed bottom pressure spectra show a large $(O(10^2))$ increase in forced wave energy levels over only a few hours. Estimates of the frequency-directional spectrum of free sea and swell were extracted from the mid-depth array data, before and after this large increase in forced wave energy levels. The estimates show nearly unidirectional free waves when forced wave energy levels were low, and seas travelling in opposing directions when forced wave energy levels were high. Theoretical predictions of forced wave energy spectra, obtained using the estimated free wave directional spectra, confirm that the observed forced waves are generated by the interactions of 0.15 - 0.3 Hz seas travelling in much different directions. The observed large fluctuations in forced wave energy levels are in good agreement with the theoretical predictions. Estimates of average wave numbers confirm that sea and swell obey the dispersion relation and double sea frequency forced waves have longer wavelengths than the interacting seas. Observed third order statistics show nonlinear coupling between directionally opposing seas and forced waves with a phase relationship predicted by theory.

References

Elgar, S. and R. T. Guza, 1985: Observations of bispectra of shoaling surface gravity waves. *J. Fluid Mech., 161*, 425-448.

Hasselmann, K., 1962: On the non-linear energy transfer in a gravity-wave spectrum, Part 1. General theory. *J. Fluid Mech., 12*, 481-500.

Hasselmann, K., W. Munk and G. MacDonald, 1963: Bispectra of ocean waves, in *Times Series Analysis*, M. Rosenblatt (ed.), John Wiley, New York, 125-139.

Herbers, T. H. C., and R. T. Guza, 1990a: Estimation of directional wave spectra from multi-component observations. *J. Phys. Oceanogr.*, in press.

Herbers, T. H. C., and R. T. Guza, 1990b: Wind wave nonlinearity observed at the sea floor. Part I: Forced wave energy. Submitted to *J. Phys. Oceanogr.*

Herbers, T. H. C., and R. T. Guza, 1990c: Wind wave nonlinearity observed at the sea floor. Part II: Wave numbers and third order statistics (manuscript in preparation).

Kinsman, B., 1965: *Wind Waves: Their Generation and propagation on the ocean surface*, 676 pp., Prentice-Hall, Englewood Cliffs, N.J.

Longuet-Higgins, M. S., 1950: A theory of the origin of microseisms. *Philos. Trans. R. Soc. London, A 243*, 1-35.

Miche, M., 1944: Movements ondulatoires de la mer en profondeur constante ou decroissante. *Ann. Ponts Chaussees, 114*, 25-87, 131-164, 270-292, 396-406.

Phillips, O. M., 1960: On the dynamics of unsteady gravity waves of finite amplitude. Part 1. The elementary interactions. *J. Fluid Mech., 9*, 193-217.